ISSN 1063-7761, Journal of Experimental and Theoretical Physics, 2013, Vol. 117, No. 5, pp. 846–861. © Pleiades Publishing, Inc., 2013.
Original Russian Text © V.A. Ignatchenko, D.S. Polukhin, 2013, published in Zhurnal Eksperimental'noi i Teoreticheskoi Fiziki, 2013, Vol. 144, No. 5, pp. 972–989.

SOLIDS AND LIQUIDS

Crossing Resonance of Wave Fields in a Medium with an Inhomogeneous Coupling Parameter

V. A. Ignatchenko and D. S. Polukhin

L. V. Kirensky Institute of Physics, Siberian Branch, Russian Academy of Sciences, Krasnoyarsk, 660036 Russia
Siberian Federal University, Svobodnyi pr. 79, Krasnoyarsk, 660041 Russia
e-mail: vignatch@iph.krasn.ru, polukhin@iph.krasn.ru

Received June 4, 2013

Abstract—The dynamic susceptibilities (Green's functions) of the system of two coupled wave fields of different physical natures in a medium with an arbitrary relation between the mean value ε and rms fluctuation Δε of the coupling parameter have been examined. The self-consistent approximation involving all diagrams with noncrossing correlation lines has been developed for the case where the initial Green's function of the homogeneous medium describes the system of coupled wave fields. The analysis has been performed for spin and elastic waves. Expressions have been obtained for the diagonal elements G_{mm} and G_{uu} of the matrix Green's function, which describe spin and elastic waves in the case of magnetic and elastic excitations, and for the off-diagonal elements G_{mu} and G_{um}, which describe these waves in the case of cross excitation. Change in the forms of these elements has been numerically studied for the case of one-dimensional inhomogeneities with an increase in Δε and with a decrease in ε under the condition that the sum of the squares of these quantities is conserved: two peaks in the frequency dependences of imaginary parts of G_{mm} and G_{uu} are broadened and then joined into one broad peak; a fine structure appears in the form of narrow resonance at the vertex of the Green's function of one wave field and narrow antiresonance at the vertex of the Green's function of the other field; peaks of the fine structure are broadened and then disappear with an increase in the correlation wavenumber of the inhomogeneities of the coupling parameter; and the amplitudes of the off-diagonal elements vanish in the limit $\varepsilon \longrightarrow 0$.

DOI: 10.1134/S1063776113130049

1. INTRODUCTION

Crossing resonance appears at the crossing point of the dispersion curves of two interacting wave fields of different physical natures. Crossing resonance in a homogeneous medium is manifested in the lift of the degeneracy of the interacting wave field frequencies at this point, in the appearance of two resonance peaks in the frequency dependences of the Green's functions of both wave fields, and in the resonant enhancement of the excitation of waves of one physical nature by the waves of the other physical nature coupled to the former waves. Both the gap between the energy levels in the spectrum and the spacing between the maxima of each Green's function, is determined by the coupling parameter ε between the wave fields.

Crossing resonance in an inhomogeneous medium was studied in the Bourret approximation [1, 2] (single scattering of waves from inhomogeneities) in [3–5] for the extremely inhomogeneous model of the interaction between two wave fields, where the coupling parameter between the fields is a random function of the coordinates with zero mean value. In this case, the interaction between the fields is due only to spatial fluctuations of this parameter. Disorder-induced crossing resonance, i.e., the lift of degeneracy and the formation of a gap in the spectrum at the crossing point of dispersion curves of wave fields, was predicted. In contrast to crossing resonance in the homogeneous medium, the gap in this case is determined by the rms fluctuation Δε of the coupling parameter.

In [6–8], we considered the same model with the inclusion of the multiple scattering of waves from inhomogeneities of the coupling parameter with zero mean value. The well-known self-consistent approximation involving all diagrams with noncrossing correlation lines has been generalized to the case of stochastically interacting wave fields. The results obtained including the processes of multiple scattering of waves from inhomogeneities are qualitatively new. Instead of the lift of the degeneracy of the wave frequencies and the splitting of resonance peaks of dynamic susceptibilities at the crossing point of the unperturbed dispersion curves, a wide single-mode resonance peak should be observed in each Green's function. The fine structure appears at the vertices of these wide peaks in the form of a narrow resonance in the Green's-function curve of one field and a narrow antiresonance at the vertex of the Green's-function curve of the other field.

In view of the results obtained in [6–8], it can be expected that the inclusion of multiple scattering of

waves also leads to significant qualitative changes in the results obtained in the Bourret approximation for the general situation, where both the rms fluctuation $\Delta\varepsilon$ and mean value ε of the coupling parameter between two wave fields are nonzero [9].

The aim of this work is to generalize the self-consistent approximation to the case of an arbitrary relation between the mean value and standard deviation of the coupling parameter between two wave fields of different physical natures and to study changes in the elements of the Green's function matrix with variation of this relation from the situation corresponding to the homogeneous case ($\varepsilon \neq 0$, $\Delta\varepsilon = 0$) to the situation corresponding to the extremely stochastic interaction ($\varepsilon = 0$, $\Delta\varepsilon \neq 0$).

As in [6–8], we study a model problem corresponding to the interaction between spin and scalar elastic waves.

The paper is organized as follows. The system of coupled equations for the Green's functions of spin and elastic waves is derived in Section 2. The self-consistent approximation for one wave field is discussed in Section 3, where the self-consistent approximation for two interacting wave fields in a medium with the inhomogeneous coupling parameter between the fields is also derived. The numerical analysis of the dependence of the elements of the matrix Green's function on the ratio of the mean value and rms fluctuation of the coupling parameter is given in Section 4. The results are summarized and discussed in Section 5.

2. SYSTEM OF EQUATIONS FOR GREEN'S FUNCTIONS

We consider the model of a ferromagnet where only the magnetostriction parameter $\varepsilon(\mathbf{x})$ ($\mathbf{x} = \{x, y, x\}$) is inhomogeneous. The equations of motion for this medium include the Landau–Lifshitz equation for the magnetization vector $\mathbf{M}$ and the equation of motion of the theory of elasticity for the elastic displacement vector $\mathbf{u}$:

$$\dot{\mathbf{M}} = -g[\mathbf{M} \times \mathbf{H}^e], \tag{1}$$

$$p\ddot{u}_i = \partial\sigma_{ij}/\partial x_j + f_i, \tag{2}$$

where g is the gyromagnetic ratio, p is the density of the medium, and σ_{ij} is the stress tensor, where $i, j = x, y, z$, and $\mathbf{f} = \mathbf{f}(\mathbf{x}, t)$ is the external mass force. The effective magnetic field $\mathbf{H}^e$ and stress tensor σ_{ij} have the form

$$\mathbf{H}^e = -\frac{\partial\mathcal{H}}{\partial\mathbf{M}} + \frac{\partial}{\partial\mathbf{x}}\frac{\partial\mathcal{H}}{\partial(\partial\mathbf{M}/\partial\mathbf{x})}, \tag{3}$$

$$\sigma_{ij} = \frac{\partial\mathcal{H}}{\partial u_{ij}}, \tag{4}$$

where $u_{ij} = (\partial u_i/\partial x_j + \partial u_j/\partial x_i)/2$ is the elastic strain tensor. The energy density $\mathcal{H}$ is written in the form

$$\mathcal{H} = \frac{\alpha}{2}\left(\frac{\partial\mathbf{M}}{\partial\mathbf{x}}\right)^2 - \mathbf{M}\cdot\mathbf{H} + \frac{\lambda u_{ii}^2}{2} + \mu u_{ij}^2 + \varepsilon(\mathbf{x})M_iM_ju_{ij}. \tag{5}$$

Here, α is the exchange parameter, λ and μ are the elastic force constants, and $\mathbf{H} = H_0\mathbf{e}_z + \mathbf{h}$, where H_0 is the external static magnetic field along the z axis and $\mathbf{h}$ is the external ac magnetic field perpendicular to the z axis. The magnetoelastic parameter $\varepsilon(\mathbf{x})$ can be represented in the form

$$\varepsilon(\mathbf{x}) = \varepsilon + \Delta\varepsilon\rho(\mathbf{x}), \tag{6}$$

where ε and $\Delta\varepsilon$ are the mean value and rms fluctuation of this parameter, respectively, and $\rho(\mathbf{x})$ is a centered ($\langle\rho(\mathbf{x})\rangle = 0$) normalized ($\langle\rho^2(\mathbf{x})\rangle = 1$) random function of the coordinates. Angle brackets stand for averaging over the ensemble of the realizations of the corresponding random function.

The stochastic properties of $\rho(\mathbf{x})$ are characterized by the correlation function depending on the difference $\mathbf{r} = \mathbf{x} - \mathbf{x}'$,

$$K(\mathbf{r}) = \langle\rho(\mathbf{x})\rho(\mathbf{x}+\mathbf{r})\rangle \tag{7}$$

or by the Fourier transform of the correlation function, i.e., the spectral density

$$S(\mathbf{k}) = \frac{1}{(2\pi)^d}\int K(\mathbf{r})e^{-i\mathbf{k}\cdot\mathbf{r}}d\mathbf{r}, \tag{8}$$

where d is the dimension of the space.

The substitution of energy density (5) into equations of motion (1) and (2) provides the following coupled system of equations for the magnetization $\mathbf{M}$ and displacement $\mathbf{u}$:

$$-\frac{\dot{\mathbf{M}}}{g} = \left[\mathbf{M}\times\left\{\alpha\Delta\mathbf{M} + \mathbf{H} - \varepsilon(\mathbf{x})M_j\left(\frac{\partial\mathbf{u}}{\partial x_j} + \frac{\partial u_j}{\partial\mathbf{x}}\right)\right\}\right], \tag{9}$$

$$\ddot{\mathbf{u}} = v_t^2\Delta\mathbf{u} + (v_l^2 - v_t^2)\mathrm{grad}\,\mathrm{div}\mathbf{u} + \frac{1}{p}\frac{\partial}{\partial x_j}(\varepsilon(\mathbf{x})M_j\mathbf{M}) + \frac{\mathbf{f}}{p}, \tag{10}$$

where $v_l = \sqrt{(\lambda + 2\mu)/p}$ and $v_t = \sqrt{\mu/p}$ are the longitudinal and transverse components of the velocity of elastic waves, respectively.

We linearize Landau–Lifshitz equation (9) in the usual way ($M_z \approx M$; $M_x, M_y \ll M$) and consider a model problem for elastic waves, where the condition $u_z = 0$, as well as the condition $v_l = v_t = v_u$, is imposed. Supposing $M_x, M_y \propto \exp(i\omega t)$ and introducing circular projections

$$m^{\pm} = M_x \pm iM_y, \quad h^{\pm} = h_x \pm ih_y, \quad u^{\pm} = u_x \pm iu_y, \quad f^{\pm} = f_x \pm if_y, \tag{11}$$

we arrive at the following coupled system of two scalar equations for resonance projections m^+ and u^+ (below, the superscript + will be omitted):

$$\alpha(\nabla^2 + \nu_m)m - \varepsilon M\frac{\partial u}{\partial z} - (\Delta\varepsilon)M\rho(\mathbf{x})\frac{\partial u}{\partial z} = -h, \quad (12)$$

$$\mu(\nabla^2 + \nu_u)u + \varepsilon M\frac{\partial m}{\partial z} + (\Delta\varepsilon)M\frac{\partial}{\partial z}(\rho(\mathbf{x})m) = -f. \quad (13)$$

Here,

$$\nu_m = \frac{\omega - \omega_0}{\alpha g M}, \quad \nu_u = \frac{\omega^2}{v_u^2}, \quad (14)$$

where ω_0 is the frequency of the homogeneous ferromagnetic resonance, which depends on the magnetic field and the demagnetizing factors of the sample and $v_u = v_t = \sqrt{\mu/p}$ is the velocity of the elastic wave.

We represent the system of Eqs. (12) and (13) in the matrix form

$$[\hat{L}(\mathbf{x}) - \hat{R}(\mathbf{x})]\hat{X}(\mathbf{x}) = \hat{F}(\mathbf{x}), \quad (15)$$

where

$$\hat{L}(\mathbf{x}) = \begin{bmatrix} \nabla^2 + \nu_m & -\dfrac{\varepsilon M}{\mu}\dfrac{\partial}{\partial z} \\ \dfrac{\varepsilon M}{\alpha}\dfrac{\partial}{\partial z} & \nabla^2 + \nu_u \end{bmatrix}, \quad (16)$$

$$\hat{R}(\mathbf{x}) = \begin{bmatrix} 0 & \dfrac{\Delta\varepsilon}{\mu}M\rho(\mathbf{x})\dfrac{\partial}{\partial z} \\ -\dfrac{\Delta\varepsilon}{\alpha}M\left(\dfrac{\partial}{\partial z}\rho(\mathbf{x}) + \rho(\mathbf{x})\dfrac{\partial}{\partial z}\right) & 0 \end{bmatrix}, \quad (17)$$

$$\hat{X}(\mathbf{x}) = \begin{bmatrix} \alpha m \\ \mu u \end{bmatrix}, \quad \hat{F}(\mathbf{x}) = \begin{bmatrix} -h \\ -f \end{bmatrix}. \quad (18)$$

It can be seen in this representation that αm and μu are the normalized variable for the coupled system of equations. This normalization is used for the matrix Green's function satisfying the equation

$$[\hat{L}(\mathbf{x}) - \hat{R}(\mathbf{x})]\hat{G}(\mathbf{x}, \mathbf{x}_0) = \delta(\mathbf{x} - \mathbf{x}_0)\hat{E}. \quad (19)$$

Here,

$$\hat{G}(\mathbf{x}, \mathbf{x}_0) = \begin{bmatrix} G_{mm}(\mathbf{x}, \mathbf{x}_0) & G_{mu}(\mathbf{x}, \mathbf{x}_0) \\ G_{um}(\mathbf{x}, \mathbf{x}_0) & G_{uu}(\mathbf{x}, \mathbf{x}_0) \end{bmatrix}, \quad (20)$$

where G_{mm} and G_{mu} (G_{uu} and G_{um}) are the spin (elastic) Green's functions at the magnetic and elastic point excitations, respectively, and

$$\hat{E} = \begin{bmatrix} 1 & 0 \\ 0 & 1 \end{bmatrix} \quad (21)$$

is the identity matrix.

We represent the Green's functions $\hat{G}$ in the form

$$\hat{G} = \hat{G}_0 + \hat{G}', \quad (22)$$

where $\hat{G}_0$ is the initial Green's function and $\hat{G}'$ is the correction caused by the inhomogeneous coupling parameter.

The substitution of Eq. (22) into Eq. (19) gives the following equations for $\hat{G}_0$ and $\hat{G}'$:

$$\hat{L}(\mathbf{x})\hat{G}_0(\mathbf{x}, \mathbf{x}_0) = \delta(\mathbf{x} - \mathbf{x}_0)\hat{E}, \quad (23)$$

$$\hat{L}(\mathbf{x})\hat{G}'(\mathbf{x}, \mathbf{x}_0) = \hat{R}(\mathbf{x})\hat{G}(\mathbf{x}, \mathbf{x}_0). \quad (24)$$

Equation (23) for the initial Green's function can be solved exactly. We analyze this solution below. Here, we only note that, according to the form of the operator $\hat{L}$, the initial Green's function $\hat{G}_0(\mathbf{x}, \mathbf{x}_0)$ describes coupled magnetoelastic waves in a homogeneous medium. Thus, in contrast to single-field situations and to the case of the stochastic interaction between wave fields ($\varepsilon = 0$, $\Delta\varepsilon \neq 0$), which was considered in [6–8], the Green's function formalism in this case is developed against the background of the initial system of coupled wave fields.

We now analyze Eq. (24) for the correction $\hat{G}'(\mathbf{x}, \mathbf{x}_0)$. According to the general rules, the formal solution of Eq. (24) can be generally represented in the form of the integral of the product of the unperturbed Green's function and right-hand side of this equation. The substitution of this solution into Eq. (22) gives the generating integral equation for the matrix Green's function $\hat{G}$:

$$\hat{G}(\mathbf{x}, \mathbf{x}_0) = \hat{G}_0(\mathbf{x}, \mathbf{x}_0) + \int\hat{G}_0(\mathbf{x}, \mathbf{x}')\hat{R}(\mathbf{x}')\hat{G}(\mathbf{x}', \mathbf{x}_0)d\mathbf{x}'. \quad (25)$$

It is inconvenient for subsequent calculations that the elements of the matrix $\hat{R}$ contain the derivatives of the random function $\rho(\mathbf{x})$. For this reason, we transform the integral in Eq. (25) through integration by parts, as was made earlier in [8, 10], and finally arrive at the generating integral equation for the matrix Green's function $\hat{G}$ in the form

$$\hat{G}(\mathbf{x}, \mathbf{x}_0) = \hat{G}_0(\mathbf{x}, \mathbf{x}_0) + \gamma\int\hat{Y}_0(\mathbf{x}, \mathbf{x}')\hat{P}(\mathbf{x}')\hat{G}(\mathbf{x}', \mathbf{x}_0)d\mathbf{x}'. \quad (26)$$

Here,

$$\hat{Y}_0(\mathbf{x}, \mathbf{x}') = \begin{bmatrix} G^0_{mm}(\mathbf{x}, \mathbf{x}') & \sqrt{\dfrac{\mu}{\alpha}}\dfrac{\partial G^0_{mu}(\mathbf{x}, \mathbf{x}')}{\partial z'} \\ G^0_{um}(\mathbf{x}, \mathbf{x}') & \sqrt{\dfrac{\mu}{\alpha}}\dfrac{\partial G^0_{uu}(\mathbf{x}, \mathbf{x}')}{\partial z'} \end{bmatrix}, \quad (27)$$

$$\hat{P}(\mathbf{x}') = \begin{bmatrix} 0 & \sqrt{\frac{\alpha}{\mu}}\rho(\mathbf{x}')\frac{\partial}{\partial z'} \\ \rho(\mathbf{x}') & 0 \end{bmatrix}, \quad (28)$$

$$\gamma = \frac{\Delta\varepsilon}{\sqrt{\alpha\mu}}M. \quad (29)$$

Using the usual procedure of successive iterations of Eq. (26), we obtain an infinite series for the matrix Green's function $\hat{G}(\mathbf{x}, \mathbf{x}_0)$. Averaging this series over the ensemble of the realizations of the random functions $\rho(\mathbf{x})$ and decoupling correlation functions using the Gauss formula, we obtain the perturbation series for the averaged Green's functions. The matrix Dyson equation is obtained from these series in the form

$$\hat{\bar{G}}(\mathbf{x}, \mathbf{x}_0) = \hat{G}_0(\mathbf{x}, \mathbf{x}_0) + \iint \hat{Y}_0(\mathbf{x}, \mathbf{x}')\hat{Q}(\mathbf{x}', \mathbf{x}'')\hat{\bar{Y}}(\mathbf{x}'', \mathbf{x}_0)d\mathbf{x}'d\mathbf{x}'', \quad (30)$$

where the mass operator (self-energy) has the form

$$\hat{Q}(\mathbf{x}', \mathbf{x}'') = \gamma^2\hat{X}_0(\mathbf{x}', \mathbf{x}'')J \cdot K(\mathbf{x}', \mathbf{x}'') + \gamma^4 \iint \hat{X}_0(\mathbf{x}', \mathbf{x}_1)\hat{X}_0(\mathbf{x}_1, \mathbf{x}_2)\hat{X}_0(\mathbf{x}_2, \mathbf{x}'')J \times [K(\mathbf{x}', \mathbf{x}_2)K(\mathbf{x}_1, \mathbf{x}'') + K(\mathbf{x}', \mathbf{x}'')K(\mathbf{x}_1, \mathbf{x}_2)] \times d\mathbf{x}_1 d\mathbf{x}_2 + \ldots. \quad (31)$$

Here, the elements of the matrices $\hat{X}_0$ are the initial Green's functions and their spatial derivatives, whereas the elements of the matrices $\hat{\bar{Y}}$ are the desired averaged Green's functions and their spatial derivatives:

$$\hat{X}_0(\mathbf{x}', \mathbf{x}'') = \begin{bmatrix} \sqrt{\frac{\mu}{\alpha}}\frac{\partial G^0_{um}(\mathbf{x}', \mathbf{x}'')}{\partial z'} & \frac{\partial^2 G^0_{uu}(\mathbf{x}', \mathbf{x}'')}{\partial z'\partial z''} \\ \hat{G}^0_{mm}(\mathbf{x}', \mathbf{x}'') & \sqrt{\frac{\alpha}{\mu}}\frac{\partial G^0_{mu}(\mathbf{x}', \mathbf{x}'')}{\partial z''} \end{bmatrix}, \quad (32)$$

$$\hat{\bar{Y}}(\mathbf{x}'', \mathbf{x}_0) = \begin{bmatrix} \bar{G}_{mm}(\mathbf{x}'', \mathbf{x}_0) & \bar{G}_{mu}(\mathbf{x}'', \mathbf{x}_0) \\ \sqrt{\frac{\alpha}{\mu}}\frac{\partial \bar{G}_{um}(\mathbf{x}'', \mathbf{x}_0)}{\partial z''} & \sqrt{\frac{\alpha}{\mu}}\frac{\partial \bar{G}_{uu}(\mathbf{x}'', \mathbf{x}_0)}{\partial z''} \end{bmatrix}, \quad (33)$$

$$J = \begin{bmatrix} 0 & 1 \\ 1 & 0 \end{bmatrix}, \quad (34)$$

and $K(\mathbf{x}', \mathbf{x}'') \equiv K(\mathbf{x}' - \mathbf{x}'')$ is the correlation function given by Eq. (7).

The diagrams of the matrix elements of the Green's functions and mass operators are shown in Fig. 1. The matrix elements of Dyson equation (30) in the diagram representation are shown in Fig. 2. It can be seen that each of four elements of the Green's functions is

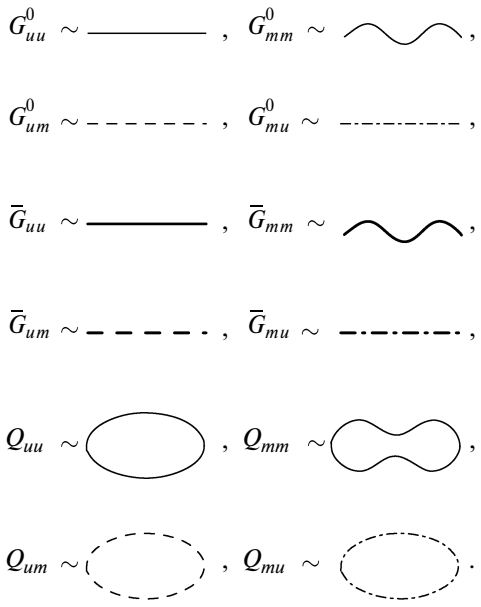

Fig. 1. Diagram notation of the elements of the matrix Green's functions $\hat{G}_0$ and $\hat{\bar{G}}$ and mass operator $\hat{Q}$.

expressed in terms of all four elements of the matrix mass operator.

We write the above relations in the **k** space. All quantities in the randomly homogeneous medium depend only on the difference $\mathbf{r} = \mathbf{x} - \mathbf{x}'$. Consequently, the Fourier transforms of all quantities have the form

$$\hat{\bar{G}}(\mathbf{r}) = \int \hat{\bar{G}}(\mathbf{k})e^{i\mathbf{k}\cdot\mathbf{r}}d\mathbf{k}, \quad \hat{\bar{G}}(\mathbf{k}) = \frac{1}{(2\pi)^d}\int \hat{\bar{G}}(\mathbf{r})e^{-i\mathbf{k}\cdot\mathbf{r}}d\mathbf{r}, \text{ etc.} \quad (35)$$

The solution of Eq. (23) for the initial Green's function in the **k** space has the form

$$\hat{G}_0(\mathbf{k}) = \begin{bmatrix} G^0_{mm}(\mathbf{k}) & iG^0_{mu}(\mathbf{k}) \\ -iG^0_{um}(\mathbf{k}) & G^0_{uu}(\mathbf{k}) \end{bmatrix}, \quad (36)$$

where

$$G^0_{mm}(\mathbf{k}) = \frac{\nu_u - k^2}{(2\pi)^d D^0}, \quad G^0_{mu}(\mathbf{k}) = \frac{(\varepsilon/\mu)Mk_z}{(2\pi)^d D^0}, \quad G^0_{um}(\mathbf{k}) = \frac{(\varepsilon/\alpha)Mk_z}{(2\pi)^d D^0}, \quad G^0_{uu}(\mathbf{k}) = \frac{\nu_m - k^2}{(2\pi)^d D^0}, \quad (37)$$

D^0 is the determinant of the system of Eqs. (12) and (13), which couples the spin and elastic waves in a united system of magnetoelastic waves:

$$D^0 = (\nu_m - k^2)(\nu_u - k^2) - \gamma_0^2 k_z^2, \quad (38)$$

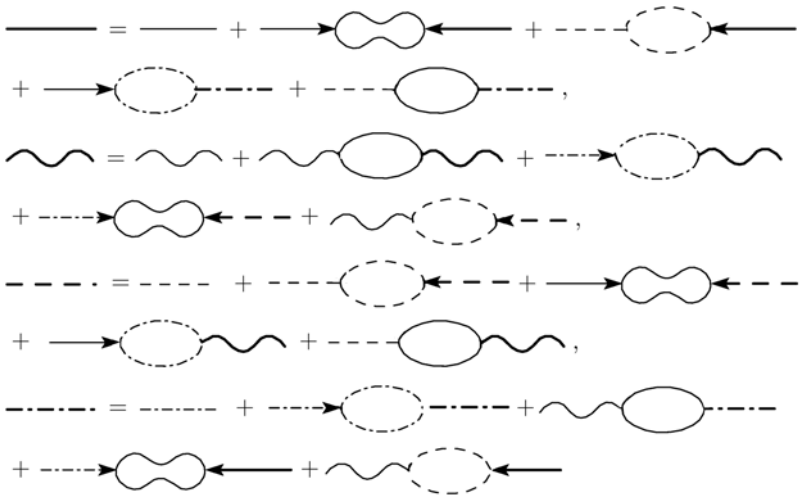

Fig. 2. Diagram representations for the matrix elements of Dyson equation (30). The arrows indicate the points at which the derivatives are calculated.

$$\gamma_0 = \frac{\varepsilon}{\sqrt{\alpha\mu}}M. \tag{39}$$

For the one-dimensional case ($k_z = k$, $d = 1$), the elements of the initial Green's function in the **r** space can be found in an explicit form from Eqs. (37). To this end, we represent D^0 in the form

$$D^0 = (k^2 - h_1^2)(k^2 - h_2^2), \tag{40}$$

where

$$h_1 = \pm\sqrt{0.5[\nu_u + \nu_m + \gamma_0^2 + \sqrt{(\nu_u + \nu_m + \gamma_0^2)^2 - 4\nu_u\nu_m}]},$$
$$h_2 = \pm\sqrt{0.5[\nu_u + \nu_m + \gamma_0^2 - \sqrt{(\nu_u + \nu_m + \gamma_0^2)^2 - 4\nu_u\nu_m}]}. \tag{41}$$

In this case, each element of matrix (36) can be written in the form of the sum of two fractions:

$$\begin{bmatrix} G^0_{mm}(k) \\ G^0_{uu}(k) \end{bmatrix} = \frac{1}{2\pi(h_2^2 - h_1^2)}\left\{\begin{bmatrix} h_1^2 - \nu_u \\ h_1^2 - \nu_m \end{bmatrix}\right.$$
$$\left.\times\frac{1}{k^2 - h_1^2} + \begin{bmatrix} \nu_u - h_2^2 \\ \nu_m - h_2^2 \end{bmatrix}\frac{1}{k^2 - h_2^2}\right\},$$
$$\begin{bmatrix} G^0_{mu}(k) \\ G^0_{um}(k) \end{bmatrix} = \frac{\varepsilon Mk}{2\pi(h_2^2 - h_1^2)}$$
$$\times\left(-\frac{1}{k^2 - h_1^2} + \frac{1}{k^2 - h_2^2}\right)\begin{bmatrix} 1/\mu \\ 1/\alpha \end{bmatrix}. \tag{42}$$

The inverse Fourier transform of Eqs. (42) gives the matrix elements of the Green's function in the homogeneous medium in the form

$$\begin{bmatrix} G^0_{mm}(r) \\ G^0_{uu}(r) \end{bmatrix} = \frac{ie^{ih_1 r}}{2h_1(h_2^2 - h_1^2)}\begin{bmatrix} h_1^2 - \nu_u \\ h_1^2 - \nu_m \end{bmatrix}$$
$$+\frac{ie^{ih_2 r}}{2h_2(h_2^2 - h_1^2)}\begin{bmatrix} \nu_u - h_2^2 \\ \nu_m - h_2^2 \end{bmatrix}, \tag{43}$$
$$\begin{bmatrix} G^0_{mu}(r) \\ G^0_{um}(r) \end{bmatrix} = \frac{\varepsilon Mi(e^{ih_2 r} - e^{ih_1 r})}{2(h_2^2 - h_1^2)}\begin{bmatrix} 1/\mu \\ 1/\alpha \end{bmatrix},$$

where $r = |x' - x''|$.

The frequency spectrum of magnetoelastic waves in the homogeneous medium was analyzed in [11–17]. The main features of this spectrum are the lift of degeneracy of frequencies of spin and elastic waves at the crossing point of their unperturbed dispersion curves ($k = k_r$, $\omega = \omega_r$) and the appearance of a gap in the spectrum of coupled waves whose width Λ is proportional to the coupling parameter ε,

$$\Lambda = \omega^+ - \omega^- = \frac{\varepsilon M}{\sqrt{\mu}}\sqrt{2\omega_M\omega_r}, \tag{44}$$

where $\omega_M = gM$.

Expression (36) describes the form of the matrix elements of the initial Green's function. The introduction of arbitrarily small damping results in the appearance of imaginary components in these elements. In this case, the imaginary part of each diagonal element of the matrix Green's function, $G^0_{mm}(\omega)$

and $G^0_{uu}(\omega)$, at $k = k_r$ has two separated peaks at the points $\omega^{\pm}$ with the spacing Λ between them.

The amplitudes of the spin (m) and elastic (u) waves in the homogeneous case ($\varepsilon \neq 0$, $\Delta\varepsilon = 0$) are expressed in terms of the initial matrix Green's function as

$$\hat{X}(\mathbf{x}) = \int \hat{G}_0(\mathbf{x}, \mathbf{x}_0)\hat{F}(\mathbf{x}_0)d\mathbf{x}_0 \quad (45)$$

in the **r** space and

$$\hat{X}(\mathbf{k}) = (2\pi)^d \hat{G}_0(\mathbf{k})\hat{F}(\mathbf{k}) \quad (46)$$

in the **k** space, where

$$\hat{X}(\mathbf{x}) = \begin{bmatrix} \alpha m(\mathbf{x}) \\ \mu u(\mathbf{x}) \end{bmatrix}, \quad \hat{F}(\mathbf{x}_0) = \begin{bmatrix} -h(\mathbf{x}_0) \\ -f(\mathbf{x}_0) \end{bmatrix}, \quad (47)$$

$$\hat{X}(\mathbf{k}) = \begin{bmatrix} \alpha m(\mathbf{k}) \\ \mu u(\mathbf{k}) \end{bmatrix}, \quad \hat{F}(\mathbf{k}) = \begin{bmatrix} -h(\mathbf{h}) \\ -f(\mathbf{k}) \end{bmatrix}. \quad (48)$$

The amplitudes $m(\mathbf{k})$ and $u(\mathbf{k})$ can be written in the explicit form

$$\begin{aligned} m(\mathbf{k}) &= -\frac{(2\pi)^d}{\alpha}[G^0_{mm}(\mathbf{k})h(\mathbf{k}) + iG^0_{mu}(\mathbf{k})f(\mathbf{k})], \\ u(\mathbf{k}) &= -\frac{(2\pi)^d}{\mu}[G^0_{uu}(\mathbf{k})f(\mathbf{k}) - iG^0_{um}(\mathbf{k})h(\mathbf{k})]. \end{aligned} \quad (49)$$

According to Eqs. (47) and (48), the normalization of the Green's functions in this work differs from the normalization of formulas in [8]. For agreement between these normalizations, quantities α and μ in Eqs. (15), (16), (22), (23), and (27)–(30) in [8] should be interchanged, i.e., $\alpha \longrightarrow \mu$, $\mu \longrightarrow \alpha$. This does not concern the other formulas in [8] and the results obtained in that work, which are valid in the new normalization.

After some algebra, the matrix Dyson equation for the total Green's function given by Eq. (30) in the **k** space has the form

$$\hat{\bar{G}}(\mathbf{k}) = \frac{\hat{E}}{\hat{G}_0^{-1}(\mathbf{k}) - (2\pi)^{2d}\hat{E}_1(\mathbf{k})\hat{Q}(\mathbf{k})\hat{E}_2(\mathbf{k})}, \quad (50)$$

where

$$\hat{\bar{G}}(\mathbf{k}) = \begin{bmatrix} \bar{G}_{mm}(\mathbf{k}) & i\bar{G}_{mu}(\mathbf{k}) \\ -i\bar{G}_{um}(\mathbf{k}) & \bar{G}_{uu}(\mathbf{k}) \end{bmatrix}, \quad (51)$$

$$\hat{Q}(\mathbf{k}) = \begin{bmatrix} Q_{uu}(\mathbf{k}) & Q_{um}(\mathbf{k}) \\ Q_{mu}(\mathbf{k}) & Q_{mm}(\mathbf{k}) \end{bmatrix}, \quad (52)$$

$$\hat{E}_1(\mathbf{k}) = \begin{bmatrix} 1 & 0 \\ 0 & -\sqrt{\mu/\alpha}ik_z \end{bmatrix}, \quad \hat{E}_2(\mathbf{k}) = \begin{bmatrix} 1 & 0 \\ 0 & \sqrt{\alpha/\mu}ik_z \end{bmatrix}. \quad (53)$$

We emphasize that the Fourier transforms of the off-diagonal elements of matrix (51) are written in the form of the product of an imaginary unit by $\bar{G}_{mu}(\mathbf{k})$ and $\bar{G}_{um}(\mathbf{k})$, and the matrix $\hat{Q}(\mathbf{k})$ has the form where the positions of the elements $Q_{ij}(\mathbf{k})$ differ from the positions of the elements in the matrix $\hat{\bar{G}}(\mathbf{k})$. The amplitudes m and u are expressed in terms of the matrix Green's functions $\hat{\bar{G}}(\mathbf{x}, \mathbf{x}_0)$ and $\hat{\bar{G}}(\mathbf{k})$ similar to Eqs. (45)–(49).

Similar to [8], we seek an expression for the mass operator $\hat{Q}(\mathbf{k})$ in the self-consistent approximation. To this end, the noncrossing correlation approximation (see below) should be generalized to the case where the initial Green's function $\hat{G}_0(\mathbf{k})$ in the uniform space describes coupled wave fields of different physical natures.

3. SELF-CONSISTENT APPROXIMATION FOR TWO COUPLED WAVE FIELDS

Before deriving the self-consistent approximation for two stochastically interacting fields, we briefly recall the main stages of the derivation of a similar approximation for one wave field (these stages were discussed in more detail in [8]). This variant of the self-consistent approximation was used at the end of the 1950s and at the beginning of the 1960s for a problem that does not concern inhomogeneous media. It was proposed by Migdal [18] when studying the electron–phonon interaction in the homogeneous medium and was analyzed in detail by Pines [19, 20], Puff and Whitfield [21], and Abrikosov, Gor'kov, and Dzyaloshinskii [22].

We briefly present the key results of those works. The system of equations for electrons and photons is approximately reduced to one equation for the electron Green's function $G(x_i, x_j)$, where the points x_i and x_j are related by the electron–phonon interaction operator $D(x_i, x_j)$. As a result, the Dyson equation for the electron Green's function is obtained in the standard form

$$\begin{aligned} \bar{G}(\mathbf{x}, \mathbf{x}_0) &= G^0(\mathbf{x}, \mathbf{x}_0) \\ &+ \iint G^0(\mathbf{x}, \mathbf{x}')Q(\mathbf{x}', \mathbf{x}'')\bar{G}(\mathbf{x}'', \mathbf{x}_0)d\mathbf{x}'d\mathbf{x}''. \end{aligned} \quad (54)$$

The Migdal self-consistent approximation is based on the representation of the mass operator $Q(\mathbf{x}', \mathbf{x}'')$ in the form

$$Q(\mathbf{x}', \mathbf{x}'') \approx \bar{G}(\mathbf{x}', \mathbf{x}'')D(\mathbf{x}', \mathbf{x}''). \quad (55)$$

In the same years, a similar variant of the self-consistent approximation was independently proposed by Kraichnan [23], who studied the effect of inhomogeneities on the dynamic susceptibility of disordered systems. The derivation of this self-consistent approxi-

mation from the expansion of the vertex part of the Green's function can be found in [24]. The Dyson equation has the form of Eq. (54) and the mass operator is approximately represented in the form

$$Q(\mathbf{x}', \mathbf{x}'') \approx \gamma^2 \bar{G}(\mathbf{x}', \mathbf{x}'') K(\mathbf{x}', \mathbf{x}''), \quad (56)$$

where γ and $K(\mathbf{x}', \mathbf{x}'')$ are the rms fluctuation and normalized correlation function of inhomogeneities, respectively ($K(\mathbf{x}', \mathbf{x}') = 1$).

A similar self-consistent approximation called the self-consistent Born approximation [22, 25, 26] is used in the theory of the scattering of electrons from impurities.

Although the Migdal approximation, Kraichnan approximation, and self-consistent Born approximation were proposed for different problems, they are mathematically identical and have a common constraint: the expansion of the Green's function obtained in these approximations contains all diagrams appearing in the exact expressions for $\bar{G}(\mathbf{x}, \mathbf{x}_0)$ except for the diagrams with crossing interaction/correlation lines between different points. For this reason, as in [8], this variant will be called below the noncrossing correlation approximation (NCA), where correlations are treated in a wide sense as stochastic correlations and averaged physical interactions.

In the $\mathbf{k}$ space, the NCA is used in two different forms. The first form involves the exact representation $\bar{G}(\mathbf{k})$ in terms of the normalized mass operator $M_\mathbf{k} = (2\pi)^d Q(\mathbf{k})$,

$$\bar{G}(\mathbf{k}) = \frac{1}{(2\pi)^d} \frac{1}{\nu - k^2 - M_\mathbf{k}}, \quad (57)$$

for which the approximate self-consistency equation is derived from Eq. (55) or (56):

$$M_\mathbf{k} \approx \gamma^2 \int \frac{S(\mathbf{k} - \mathbf{k}_1) d\mathbf{k}_1}{\nu - k_1^2 - M_{\mathbf{k}_1}}, \quad (58)$$

where $S(\mathbf{k})$ is the Fourier transform of the correlation function $K(\mathbf{x}', \mathbf{x}'')$ and ν is the normalized frequency.

In the second form, Eq. (55) or (56) is substituted into Eq. (54), leading to the following approximate nonlinear integral self-consistency equation for the Green's function $\bar{G}(\mathbf{k})$:

$$\bar{G}(\mathbf{k}) \approx G^0(\mathbf{k}) + \gamma^2 (2\pi)^{2d} G^0(\mathbf{k}) \bar{G}(\mathbf{k}) \times \int S(\mathbf{k} - \mathbf{k}_1) \bar{G}(\mathbf{k}_1) d\mathbf{k}_1. \quad (59)$$

The NCA approach is widely used both in the calculations of the effects of the electron–phonon interaction (see, e.g., [27, 28]) and for various problems of hydrodynamics and stochastic radiophysics (see, e.g., [29–32]). The NCA was also generalized to the case of the inhomogeneity of nonlocal (off-diagonal) terms of the phenomenological Hamiltonian: exchange constants in ferromagnets and force constants in elastic media. The integral term of the Dyson equation in this case contains the spatial derivatives of the Green's functions rather than the functions themselves and the mass operator is a matrix whose components contain the second derivatives of the initial Green's functions [10]. We note that the authors of [10, 32] were inaccurate in terminology: they considered the NCA as a variant of another popular self-consistent approximation—the coherent potential approximation, which was proposed by Soven [33] and Taylor [34] and was further developed in numerous works (see, e.g., [35–41]).

The applicability condition of the NCA for the problem of the scattering of electrons from impurities was approximately estimated in [22, 25, 26]:

$$(k_F l)^{-1} \ll 1, \quad (60)$$

where k_F is the Fermi momentum and l is the mean free path of the electron. For the problem of the scattering of waves from impurities in the continuous medium in the case where waves in the region of a certain resonance wavenumber k_r play a dominant role, condition (60) can be transformed to the form

$$k_c / k_r \ll 1, \quad (61)$$

where k_c is the correlation wavenumber ($k_c^{-1} = r_c$ is the correlation radius of inhomogeneities). In [8], we supplemented the estimate of the applicability of the NCA, considering the limiting case $k_c = 0$, where the series for the Green's function can be summed exactly. In this case, the random functions $\rho(\mathbf{x})$ become random variables whose stochastic properties are described by a certain distribution function $f(\rho)$ (a similar model of independent grains in a polycrystal was proposed in [42] to calculate the lineshape of the ferromagnetic resonance). The distribution function $f(\rho)$ for the exact averaged Green's function is a Gaussian function (Keldysh model, see [26]) and the imaginary part of the Green's function has the form

$$G''(\nu, \mathbf{k}) = \frac{\pi}{(2\pi)^{7/2}\sigma} \exp\left(-\frac{\xi^2}{2\sigma^2}\right), \quad (62)$$

where $\xi = \nu - k^2$ and σ is the rms fluctuation of the frequency.

At the same time, the integral self-consistency equation of the NCA in the limit $k_c \longrightarrow 0$ is also solved exactly and gives the following expression for the averaged imaginary part of Green's function [32]:

$$G''_{NCA}(\nu, \mathbf{k}) = \begin{cases} \dfrac{\sqrt{(2\sigma)^2 - \xi^2}}{(2\pi)^3 2\sigma^2}, & |\xi| \le 2\sigma, \\ 0, & |\xi| > 2\sigma. \end{cases} \quad (63)$$

The forms of functions (62) and (63) differ from each other (see Fig. 5 in [8]). However, both Green's functions, exact (62) and approximate (63), give the same results for the mean frequency and its standard devia-

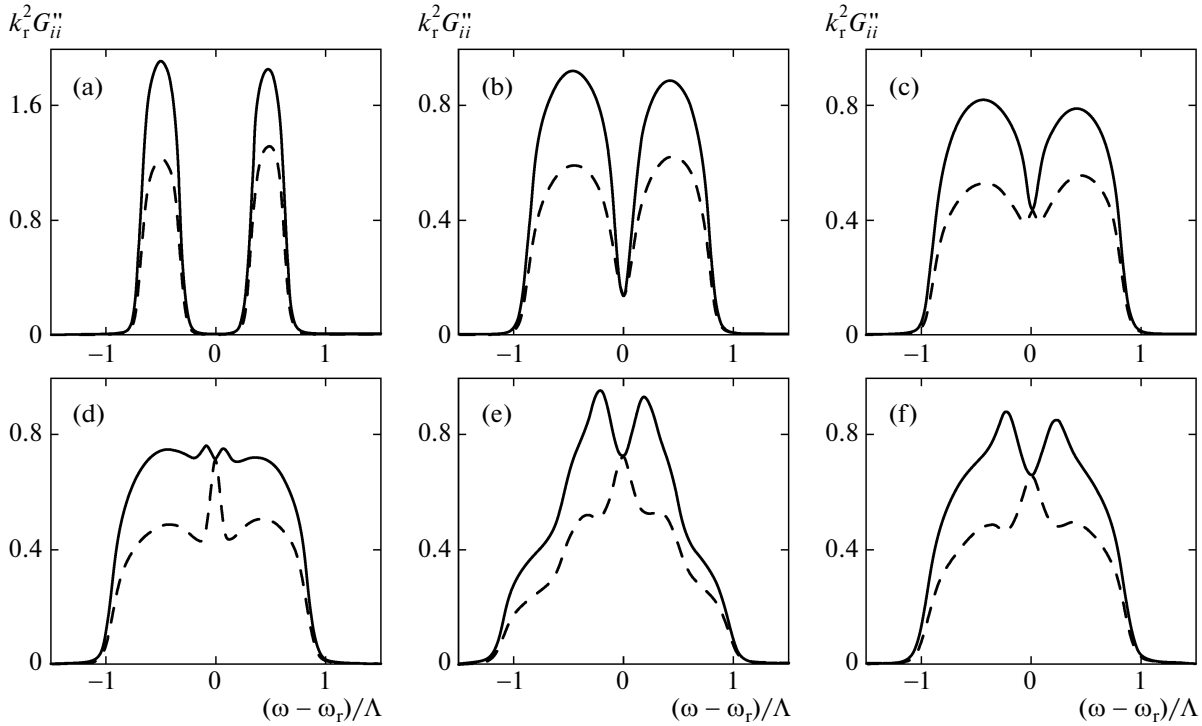

Fig. 3. Imaginary parts of the diagonal elements of the matrix Green's function of the (dashed curves) spin, $G''_{mm}(\omega)$, and (solid curves) elastic, $G''_{uu}(\omega)$, waves at $\kappa_c = k_c/k_r = 0.8 \times 10^{-2}$ for $(\varepsilon/\varepsilon_0)^2/(\Delta\varepsilon/\varepsilon)^2 =$ (a) 0.95/0.05, (b) 0.8/0.2, (c) 0.75/0.25, (d) 0.7/0.3, (e) 0.25/0.75, and (f) 0/1. The scale of the vertical axis in Fig. 3a is twice as large as the scale of the vertical axes in Figs. 3b–3f.

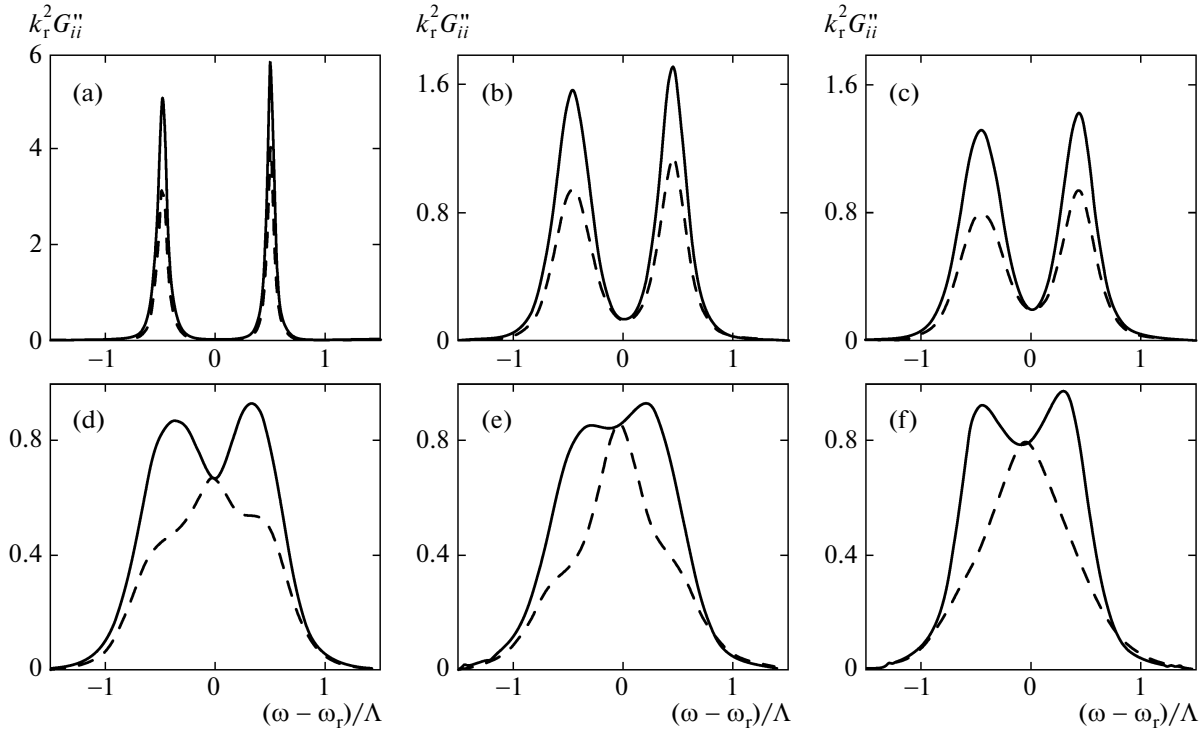

Fig. 4. Imaginary parts of the diagonal elements of the matrix Green's function of the (dashed curves) spin, $G''_{mm}(\omega)$, and (solid curves) elastic, $G''_{uu}(\omega)$, waves at $\kappa_c = k_c/k_r = 0.8 \times 10^{-2}$ for $(\varepsilon/\varepsilon_0)^2/(\Delta\varepsilon/\varepsilon)^2 =$ (a) 0.95/0.05, (b) 0.8/0.2, (c) 0.75/0.25, (d) 0.5/0.5, (e) 0.25/0.75, and (f) 0/1. The scales of the vertical axes in Figs. 4a–4c differ from the scale of these axes in Figs. 4d–3f.

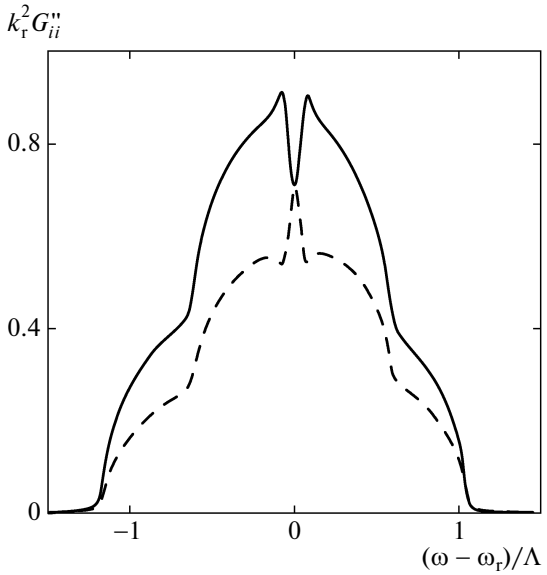

Fig. 5. Imaginary parts of the diagonal elements of the matrix Green's function of the (dashed curves) spin, $G_{mm}''(\omega)$, and (solid curves) elastic, $G_{uu}''(\omega)$, waves at $\kappa_c = 0.8 \times 10^{-3}$ for the same $\varepsilon/\Delta\varepsilon$ ratio as in Figs. 3e and 4e.

tion characterizing the half-width of the resonance line:

$$\langle \nu \rangle = k^2, \quad \sqrt{\langle (\nu - \langle \nu \rangle^2) \rangle} = \sigma. \tag{64}$$

Formulas (62) and (63) will be used below when discussing the results of this work.

In [8], we studied the stochastic interaction ($\varepsilon = 0$, $\Delta\varepsilon \neq 0$) between two wave fields. The system of coupled Dyson equations for the averaged spin, $\bar{G}_m$, and elastic, $\bar{G}_u$, Green's functions had the form

$$\begin{aligned} \bar{G}_m(\mathbf{x}, \mathbf{x}_0) &= G_m^0(\mathbf{x}, \mathbf{x}_0) \\ &+ \int\int G_m^0(\mathbf{x}, \mathbf{x}') Q_u(\mathbf{x}', \mathbf{x}'') \bar{G}_m(\mathbf{x}'', \mathbf{x}_0) d\mathbf{x}' d\mathbf{x}'', \end{aligned} \tag{65}$$

$$\begin{aligned} \bar{G}_u(\mathbf{x}, \mathbf{x}_0) &= G_u^0(\mathbf{x}, \mathbf{x}_0) \\ &+ \int\int \frac{\partial G_u^0(\mathbf{x}, \mathbf{x}')}{\partial z'} Q_m(\mathbf{x}', \mathbf{x}'') \\ &\times \frac{\partial \bar{G}_u(\mathbf{x}'', \mathbf{x}_0)}{\partial z''} d\mathbf{x}' d\mathbf{x}'', \end{aligned} \tag{66}$$

where the elastic mass operator Q_u appeared in the equation for the spin Green's function $\bar{G}_m$, whereas the spin mass operator Q_m entered into the equation for the elastic Green's function $\bar{G}_u$. To introduce the generalized NCA, these mass operators were expressed in terms of the desired Green's functions as

$$Q_m(\mathbf{x}', \mathbf{x}'') \approx \gamma^2 \bar{G}_m(\mathbf{x}', \mathbf{x}'') K(\mathbf{x}', \mathbf{x}''), \tag{67}$$

$$Q_u(\mathbf{x}', \mathbf{x}'') \approx \gamma^2 \frac{\partial^2 \bar{G}_u(\mathbf{x}', \mathbf{x}'')}{\partial z' \partial z''} K(\mathbf{x}', \mathbf{x}''). \tag{68}$$

It was shown that the substitution of these expressions into Eqs. (65) and (66) and the subsequent iteration of these equations really lead to the NCA, where the expansions of the Green's functions include all diagrams except for the diagrams with crossing correlation lines.

We now derive approximate self-consistent equations for the mass operator $\hat{Q}(\mathbf{k})$. Following the ideas proposed in [18, 23] and their development in [8, 32], we approximately express the matrix elements of the mass operator $\hat{Q}(\mathbf{x}', \mathbf{x}'')$ in terms of the elements of the desired Green's function $\hat{\bar{G}}(\mathbf{x}', \mathbf{x}'')$:

$$\begin{aligned} Q_{mm}(\mathbf{x}', \mathbf{x}'') &\approx \gamma^2 \bar{G}_{mm}(\mathbf{x}', \mathbf{x}'') K(\mathbf{x}', \mathbf{x}''), \\ Q_{uu}(\mathbf{x}', \mathbf{x}'') &\approx \gamma^2 \frac{\partial^2}{\partial z' \partial z''} \bar{G}_{uu}(\mathbf{x}', \mathbf{x}'') K(\mathbf{x}', \mathbf{x}''), \\ Q_{um}(\mathbf{x}', \mathbf{x}'') &\approx \gamma^2 \sqrt{\frac{\alpha}{\mu}} \frac{\partial}{\partial z'} \\ &\times \bar{G}_{um}(\mathbf{x}', \mathbf{x}'') K(\mathbf{x}', \mathbf{x}''), \\ Q_{mu}(\mathbf{x}', \mathbf{x}'') &\approx \gamma^2 \sqrt{\frac{\mu}{\alpha}} \frac{\partial}{\partial z''} \\ &\times \bar{G}_{mu}(\mathbf{x}', \mathbf{x}'') K(\mathbf{x}', \mathbf{x}''). \end{aligned} \tag{69}$$

The Fourier transform provides expressions for the components of the mass operator tensor in the $\mathbf{k}$ space:

$$\begin{aligned} Q_{mm}(\mathbf{k}) &\approx \gamma^2 \int \bar{G}_{mm}(\mathbf{k}_1) S(\mathbf{k} - \mathbf{k}_1) d\mathbf{k}_1, \\ Q_{uu}(\mathbf{k}) &\approx \gamma^2 \int k_{1z}^2 \bar{G}_{uu}(\mathbf{k}_1) S(\mathbf{k} - \mathbf{k}_1) d\mathbf{k}_1, \\ Q_{um}(\mathbf{k}) &\approx \gamma^2 \sqrt{\frac{\alpha}{\mu}} \int k_{1z} \bar{G}_{um}(\mathbf{k}_1) S(\mathbf{k} - \mathbf{k}_1) d\mathbf{k}_1, \\ Q_{mu}(\mathbf{k}) &\approx \gamma^2 \sqrt{\frac{\mu}{\alpha}} \int k_{1z} \bar{G}_{mu}(\mathbf{k}_1) S(\mathbf{k} - \mathbf{k}_1) d\mathbf{k}_1. \end{aligned} \tag{70}$$

The system of integral equations can be simplified by introducing one normalized mass operator instead of Q_{um} and Q_{mu}. To this end, we represent Eq. (50) in the form

$$\hat{\bar{G}}(\mathbf{k}) = \frac{1}{(2\pi)^d \det\left|\hat{\bar{G}}^{-1}(\mathbf{k})\right|} \begin{bmatrix} A_{mm} & A_{mu} \\ A_{um} & A_{uu} \end{bmatrix}, \tag{71}$$

where

$$A_{mm} = \nu_u - k^2 - (2\pi)^d k_z^2 Q_{mm}(\mathbf{k}),$$
$$A_{uu} = \nu_m - k^2 - (2\pi)^d Q_{uu}(\mathbf{k}),$$
$$A_{mu} = i\frac{\varepsilon}{\mu}Mk_z + (2\pi)^d\sqrt{\frac{\alpha}{\mu}}ik_z Q_{um}(\mathbf{k}), \quad (72)$$
$$A_{um} = -i\frac{\varepsilon}{\alpha}Mk_z - (2\pi)^d\sqrt{\frac{\mu}{\alpha}}ik_z Q_{mu}(\mathbf{k}),$$
$$\hat{\bar{G}}^{-1}(\mathbf{k}) = \begin{bmatrix} A_{uu} & -A_{mu} \\ -A_{um} & A_{mm} \end{bmatrix}. \quad (73)$$

We represent the off-diagonal elements $\bar{G}_{mu}(\mathbf{k})$ and $\bar{G}_{um}(\mathbf{k})$ of matrix (71) in the form

$$\bar{G}_{mu}(\mathbf{k}) = \frac{(\varepsilon/\mu)Mk_z(1+T_\mathbf{k})}{(2\pi)^d \det\left|\hat{\bar{G}}^{-1}(\mathbf{k})\right|}, \quad (74)$$

$$\bar{G}_{um}(\mathbf{k}) = \frac{(\varepsilon/\alpha)Mk_z(1+T_\mathbf{k})}{(2\pi)^d \det\left|\hat{\bar{G}}^{-1}(\mathbf{k})\right|}, \quad (75)$$

where

$$T_\mathbf{k} = (2\pi)^d\frac{\sqrt{\alpha\mu}}{\varepsilon M}Q_{mu}(\mathbf{k}) = (2\pi)^d\frac{\sqrt{\alpha\mu}}{\varepsilon M}Q_{um}(\mathbf{k}). \quad (76)$$

We now verify that resulting expression (76) is correct. Changing $\mathbf{k}$ to $\mathbf{k}_1$ in Eqs. (74) and (75), substituting these expressions into the integrands in Eqs. (70), and multiplying the resulting formulas for $Q_{mu}(\mathbf{k})$ and $Q_{um}(\mathbf{k})$ by $(2\pi)^d\sqrt{\alpha\mu}/\varepsilon M$, we make sure that the equations are identical. Introducing the normalized diagonal mass operators

$$M_\mathbf{k} = (2\pi)^d k_z^2 Q_{mm}(\mathbf{k}), \quad U_\mathbf{k} = (2\pi)^d Q_{uu}(\mathbf{k}), \quad (77)$$

we obtain the final form of the system of Dyson equations

$$\bar{G}_{mm}(\mathbf{k}) = \frac{\nu_u - k^2 - M_\mathbf{k}}{(2\pi)^d D_\mathbf{k}},$$
$$\bar{G}_{mu}(\mathbf{k}) = \frac{(\varepsilon/\mu)Mk_z(1+T_\mathbf{k})}{(2\pi)^d D_\mathbf{k}},$$
$$\bar{G}_{um}(\mathbf{k}) = \frac{(\varepsilon/\alpha)Mk_z(1+T_\mathbf{k})}{(2\pi)^d D_\mathbf{k}}, \quad (78)$$
$$\bar{G}_{uu}(\mathbf{k}) = \frac{\nu_m - k^2 - U_\mathbf{k}}{(2\pi)^d D_\mathbf{k}},$$

and the self-consistency equations for the mass operators $M_\mathbf{k}$, $U_\mathbf{k}$, and $T_\mathbf{k}$:

$$M_\mathbf{k} = \gamma^2 k_z^2 \int D_{\mathbf{k}_1}^{-1}(\nu_u - k_1^2 - M_{\mathbf{k}_1})S(\mathbf{k}-\mathbf{k}_1)d\mathbf{k}_1,$$
$$U_\mathbf{k} = \gamma^2 \int k_{1z}^2 D_{\mathbf{k}_1}^{-1}(\nu_m - k_1^2 - U_{\mathbf{k}_1})S(\mathbf{k}-\mathbf{k}_1)d\mathbf{k}_1, \quad (79)$$
$$T_\mathbf{k} = \gamma^2 \int k_{1z}^2 D_{\mathbf{k}_1}^{-1}(1+T_{\mathbf{k}_1})S(\mathbf{k}-\mathbf{k}_1)d\mathbf{k}_1,$$

where

$$D_{\mathbf{k}_1} = (\nu_u - k_1^2 - M_{\mathbf{k}_1})(\nu_m - k_1^2 - U_{\mathbf{k}_1}) - \gamma_0^2 k_{1z}^2(1+T_{\mathbf{k}_1})^2.$$

Since all required variables $M_\mathbf{k}$, $U_\mathbf{k}$, and $T_\mathbf{k}$ also appear in the denominator of each integrand, Eqs. (79) constitute the system of complex coupled integral equations with respect to these variables. This system can be represented in the form of a system of infinite continued fractions.

For numerical analysis, it is convenient to write Eqs. (79) in the form of recurrence formulas

$$M_\mathbf{k}^{(n)} = \gamma^2 k_z^2 \int \frac{1}{D_{\mathbf{k}_1}^{(n-1)}}(\nu_u - k_1^2 - M_{\mathbf{k}_1}^{(n-1)})S(\mathbf{k}-\mathbf{k}_1)d\mathbf{k}_1,$$
$$U_\mathbf{k}^{(n)} = \gamma^2 \int k_{1z}^2 \frac{1}{D_{\mathbf{k}_1}^{(n-1)}}(\nu_m - k_1^2 - U_{\mathbf{k}_1}^{(n-1)})S(\mathbf{k}-\mathbf{k}_1)d\mathbf{k}_1, \quad (80)$$
$$T_\mathbf{k}^{(n)} = \gamma^2 \int k_{1z}^2 \frac{1}{D_{\mathbf{k}_1}^{(n-1)}}(1+T_{\mathbf{k}_1}^{(n-1)})S(\mathbf{k}-\mathbf{k}_1)d\mathbf{k}_1,$$

where

$$D_{\mathbf{k}_1}^{(n-1)} = (\nu_u - k_1^2 - M_{\mathbf{k}_1}^{(n-1)})(\nu_m - k_1^2 - U_{\mathbf{k}_1}^{(n-1)}) - \gamma_0^2 k_{1z}^2(1+T_{\mathbf{k}_1}^{(n-1)})^2, \quad (81)$$

and superscript n is the number of terms taken into account in continued fractions.

4. STUDY OF THE ELEMENTS OF THE MATRIX GREEN'S FUNCTION

Below, we analyze system (80) only for one-dimensional inhomogeneities of the coupling parameter $\varepsilon(\mathbf{x}) = \varepsilon(z)$. In this case, $d = 1$ in Eqs. (78) and (79) and the vector $\mathbf{k}$ has only one component $k_z = k$.

Simulating the correlation properties of the random function $\rho(x)$ by an exponential correlation function, we obtain the expressions

$$K(r) = e^{-k_c r}, \quad S(k) = \frac{1}{\pi}\frac{k_c}{k_c^2 + k^2}, \quad (82)$$

for the one-dimensional case, where $r = |x - x'|$ and k_c is the correlation wavenumber of inhomogeneities ($r_c = k_c^{-1}$ is the correlation radius). We first consider the first term of a continued fraction and set $n = 1$ in Eqs. (80). In this case, these equations have the following form corresponding to the Bourret approximation [1]:

$$M_k^{(1)} = \gamma^2 k^2 \int \frac{1}{D_{k_1}^0}(\nu_u - k_1^2)S(k-k_1)dk_1,$$
$$U_k^{(1)} = \gamma^2 \int k_1^2 \frac{1}{D_{k_1}^0}(\nu_m - k_1^2)S(k-k_1)dk_1, \quad (83)$$

$$T_k^{(1)} = \gamma^2 \int k_1^2 \frac{1}{D_{k_1}^0} S(k-k_1)dk_1.$$

Changing k to k_1 in Eq. (40), we represent $D_{k_1}^0$ in the form

$$D_{k_1}^0 = (k_1^2 - h_1^2)(k_1^2 - h_2^2), \quad (84)$$

where h_1 and h_2 are given by Eqs. (41). Substituting $S(k)$ into Eqs. (83) and performing integration using the residue theorem, we obtain M_k, U_k, and T_k in the first approximation:

$$M_k^{(1)} = \gamma^2 k^2 \frac{(h_1+h_2)(h_1h_2A_u - 2\nu_u k_c^2) - ik_c\{h_1h_2A_u - \nu_u[B-(h_1+h_2)^2 + h_1^2h_2^2]\}}{(h_1+h_2)h_1h_2[(h_1-ik_c)^2 - k^2][(h_2-ik_c)^2-k^2]},$$

$$U_k^{(1)} = \gamma^2 \frac{(h_1+h_2)(A_mB - 2h_1h_2k_c^2) + ik_c\{h_1h_2A_m - B[\nu_m + (h_1+h_2)^2] + h_1^2h_2^2\}}{(h_1+h_2)[(h_1-ik_c)^2 - k^2][(h_2-ik_c)^2-k^2]}, \quad (85)$$

$$T_k^{(1)} = \gamma^2 \frac{(h_1+h_2)B - ik_c(B-h_1h_2)}{(h_1+h_2)[(h_1-ik_c)^2 - k^2][(h_2-ik_c)^2-k^2]},$$

where $A_{m,u} = \nu_{u,m} - k^2 - k_c^2$, $B = k^2 + k_c^2$. The analytical expressions for M_k, U_k, and T_k even in the first approximation contain a damping term proportional to ik_c in the denominator. For this reason, it is unnecessary to introduce an artificial damping term into Eqs. (83) to remove divergence in subsequent numerical calculations.

The substitution of Eqs. (85) into Eqs. (78) gives the elements of the matrix Green's function $\hat{\bar{G}}^{(1)}$ in the first approximation. Further, using Eqs. (80) and making successive substitutions, we obtain infinite branched continued fractions. In the numerical calculation of each next approximation n, the number of peaks in imaginary parts of the elements of Green's function (78) increases: in the first approximation at $n = 1$ (Bourret approximation), there are four peaks in each of the diagonal elements $G_{mm}(\omega)$ and $G_{uu}(\omega)$; at $n = 2$, there are six peaks; at $n = 3$, there are eight peaks; etc. The area under each curve does not change in the process of an increase in the number of successive substitutions and each curve tends to its extreme value. All below figures show the shape of the elements of the matrix Green's function corresponding to the n value ensuring the convergence of successive approximations. This n value depends on the chosen parameters of the system, primarily on k_c. For large k_c values, several successive approximations can be sufficient; for small k_c values, tens and even hundreds successive numerical integrations of recurrence relations (80) are required.

With the growth of inhomogeneities, ε decreases from its initial value ε_0 to zero and $\Delta\varepsilon$ increases from zero to a certain maximum value ε_0' which is closed to ε_0. For simplicity, we set $\varepsilon_0' = \varepsilon_0$ and analyze the form of the diagonal and off-diagonal elements of the Green's functions at the crossing-resonance point $k = k_r$ with an increase in $\Delta\varepsilon$ and with a decrease in ε with the conservation of the sum of the squares of these quantities,

$$\varepsilon^2 + (\Delta\varepsilon)^2 = \varepsilon_0^2. \quad (86)$$

Samples in which intermediate states between two extreme states—homogeneous state ($\varepsilon = \varepsilon_0$, $\Delta\varepsilon = 0$) and completely stochastic state ($\varepsilon = 0$, $\Delta\varepsilon \neq 0$)—will be experimentally implemented by varying the composition or processing method should not necessarily satisfy Eq. (86). This condition is used only for the consistent consideration of all intermediate states with any ratios $(\varepsilon/\varepsilon_0)^2$ and $(\Delta\varepsilon/\varepsilon_0)^2$.

Figure 3 shows several characteristic pictures of change in the shapes of the imaginary parts of the Green's functions (dashed lines) $G_{mm}''(\omega)$ and (solid lines) $G_{uu}''(\omega)$ with an increase in $\Delta\varepsilon$ for a small k_c value corresponding to $\kappa_c \equiv k_c/k_r = 0.8 \times 10^{-2}$. Figure 3a corresponds to the coupling parameter close to homogeneous and describes the standard splitting of each Green's function into two resonance peaks, which corresponds to the lift of degeneracy of frequencies in the spectrum of spin and elastic waves at the crossing resonance point. The peaks are spaced by Λ proportional to the coupling parameter ε. The width of the peaks is determined both by damping proportional to the correlation radius k_c and by the stochastic distribution of frequencies, which is proportional to $\Delta\varepsilon$, so that the latter contribution prevails at this relation between $\Delta\varepsilon$ and κ_c. With an increase in $\Delta\varepsilon$ (Figs. 3b, 3c), the width of the peaks, which is due to the stochastic distribution of frequencies, increases and peaks continuously approach each other until they are joined into one broad peak (Fig. 3d). A fine structure appears on the top of this broad peak: a narrow resonance is formed on the top of the wide peak of the function $G_{mm}''(\omega)$ and a narrow antiresonance is formed on the top of the wide peak of the function $G_{uu}''(\omega)$. With a further increase in $\Delta\varepsilon$ (Fig. 3e), the for-

mation of the fine structure continues and the picture similar to that studied in [8] appears at the full randomization of the system (Fig. 3f, $\Delta\varepsilon = \varepsilon_0$, $\varepsilon = 0$). It was shown in [8] that resonance and antiresonance of the fine structure have approximate mirror symmetry in the state of the full randomization of the coupling parameter. Both resonance and antiresonance lines have the widths proportional to k_c and, at small k_c values, can be much narrower than those shown in Figs. 3d–3f. With an increase in k_c, the widths of resonance and antiresonance lines of the fine structure increase, whereas the width of the wide peak decreases owing to the exchange narrowing effect. As a result, the fine structure disappears first in the function $G''_{mm}(\omega)$ and, then, in the function $G''_{uu}(\omega)$. Just the k_c value at which the fine structure for $\Delta\varepsilon = \varepsilon_0$ and $\varepsilon = 0$ should disappear only in the function $G''_{mm}(\omega)$ was chosen for the set of pictures shown in Fig. 4. The peaks of the crossing resonance in Figs. 4a–4c are much narrower and higher than those shown in Figs. 3a–3c (the scales of the vertical axes in these figures are different). This is due to the exchange narrowing effect, which is manifested in Fig. 4 stronger than in Fig. 3 owing to a larger k_c value in the former figure. With an increase in $\Delta\varepsilon$, these peaks approach each other and are broadened and the fine structure is formed (Fig. 4d) with wider resonance and antiresonance lines than those in Fig. 3. The "decomposition" of this fine structure begins in Fig. 4e, and the fine structure in the function $G''_{mm}(\omega)$ is already absent in Fig. 4f corresponding to the results of [8].

To discuss the results, we first consider the limiting case of infinite correlation radius ($k_c = 0$). In this case, $S(\mathbf{k} - \mathbf{k}_1) \longrightarrow \delta(\mathbf{k} - \mathbf{k}_1)$ in integral self-consistency equations (79) for mass operators, integrals are calculated exactly, and Eqs. (79) have the form of a system of algebraic equations:

$$\begin{aligned} M_{\mathbf{k}} &= \gamma^2 k_z^2 D_{\mathbf{k}}^{-1}(\nu_u - k^2 - M_{\mathbf{k}}), \\ U_{\mathbf{k}} &= \gamma^2 k_z^2 D_{\mathbf{k}}^{-1}(\nu_m - k^2 - U_{\mathbf{k}}), \\ T_{\mathrm{k}} &= \gamma^2 k_z^2 D_{\mathbf{k}}^{-1}(1 + T_{\mathbf{k}}). \end{aligned} \tag{87}$$

According to the first two equations in Eqs. (87),

$$M_{\mathbf{k}}(\nu_m - k^2 - U_{\mathbf{k}}) = U_{\mathbf{k}}(\nu_u - k^2 - M_{\mathbf{k}}). \tag{88}$$

Since the product $M_{\mathbf{k}}U_{\mathbf{k}}$ cancels out, it follows from Eq. (88) that

$$\frac{M_{\mathbf{k}}}{U_{\mathbf{k}}} = \frac{\nu_u - k^2}{\nu_m - k^2}. \tag{89}$$

Passing from the normalized frequencies to ω on the right-hand side of Eq. (89) and using Eqs. (78), we conclude that the ratio of the diagonal elements $\bar{G}_{mm}$ and $\bar{G}_{uu}$ at $k_c = 0$ near the crossing resonance frequency $\omega = \omega_r$ is given by the expression

$$\frac{\bar{G}_{mm}(\omega, k_r)}{\bar{G}_{uu}(\omega, k_r)} = \frac{M_{k_r}}{U_{k_r}} = \frac{v_m}{v_u}, \tag{90}$$

where $v_m = 2\alpha g M k_r$ is the velocity of spin waves in the region of crossing resonance. The inequality $v_m < v_u$ is satisfied near the first crossing point of the dispersion curves of the spin and elastic waves. Therefore, at $k_c = 0$ in this region, according to Eq. (90), we have the inequality

$$\bar{G}_{mm}(\omega) < \bar{G}_{uu}(\omega). \tag{91}$$

Thus, Eqs. (90) and (91) obtained in [8] for the case $\varepsilon = 0$ are valid for any relations between ε and $\Delta\varepsilon$.

At the same time, it can be seen in Figs. 3 and 4 that, at $k_c \neq 0$ at the point $\omega = \omega_r$, we have the other relation

$$\bar{G}_{mm}(\omega_r) = \bar{G}_{uu}(\omega_r), \tag{92}$$

whereas Eq. (91) is satisfied at all other frequencies. Thus, Eq. (92) obtained in [8] for the case $\varepsilon = 0$ and any values $k_c \neq 0$ is valid for any relations between ε and $\Delta\varepsilon$. The universality of this relation supports the assumption made in [8] that it is a consequence of the general equiprobable distribution of the energy over fluctuation oscillations of both physical fields at the crossing resonance point.

According to the results of this work, the physical picture is as follows. The value $k_c = 0$ corresponds to the model of independent grains in a polycrystal; for two interacting fields, this model is an ensemble of homogeneous samples differing only in the coupling parameter in each nth sample. The spectrum of coupled magnetoelastic fields in each sample has a gap $\Lambda_n \propto |\varepsilon_n|$ at the crossing resonance point $k = k_r$. The fields in different samples are independent of each other. The entire system is characterized by the averaged matrix Green's function $\hat{\bar{G}}(\omega, \mathbf{k})$, which depends on the averaged parameters of the system: the mean value $\varepsilon = \langle \varepsilon_n \rangle$ and the standard deviation $\Delta\varepsilon = \langle \Delta\varepsilon_n \rangle$ of the coupling parameter. The peaks of the diagonal elements $\bar{G}_{mm}(\omega, \mathbf{k})$ and $\bar{G}_{uu}(\omega, \mathbf{k})$ of the Green's function in the region of crossing resonance are spaced by $\Lambda \propto \varepsilon$ and have the width $\Delta\omega \propto \Delta\varepsilon$. Damping in the system is absent. Inequality (91) is satisfied for all frequencies inside these peaks.

At an arbitrarily small value $k_c \neq 0$, fluctuation components appear in the spin and elastic fields along with the interaction both between these components and between each of them and coherent (averaged) components of these fields. At the crossing resonance point $k = k_r$, $\omega = \omega_r$, the energy distribution over fluctuation components of both fields should be equiprobable; equality (92) obtained in numerical calculations likely follows from this equiprobable energy distribu-

tion. How are the Green's functions transformed in order to satisfy this law? This is shown in Fig. 5, which corresponds to the same parameters ε and Δε as in Figs. 3e and 4e, but corresponds to the value $\kappa_c = 0.8 \times 10^{-3}$, which is an order of magnitude smaller than that in Fig. 3e. The function $\bar{G}''_{mm}(\omega)$ "raises" a thin "feeler" (fine-structure resonance) at the point $\omega = \omega_r$, whereas the function $\bar{G}''_{uu}(\omega)$ "drops" a similar feeler (fine-structure antiresonance) at the same point. These feelers touch each other between the maxima of wide peaks of both functions, and the required equality is satisfied at the point $\omega = \omega_r$. The inequality $\bar{G}''_{mm}(\omega) < \bar{G}''_{uu}(\omega)$ remains valid for all other frequencies except for $\omega = \omega_r$ and the shape of the functions remains almost unchanged compared to the case $k_c = 0$. In view of this interpretation, the fast formation of the fine structure with an increase in Δε is natural: the fine structure should appear as soon as the difference between the functions $\bar{G}''_{mm}(\omega)$ and $\bar{G}''_{uu}(\omega)$ near $\omega = \omega_r$ becomes noticeable. The fine structure appears in Fig. 3d already at $(\Delta\varepsilon/\varepsilon_0)^2 = 0.3$ and is well developed in Fig. 4d at $(\Delta\varepsilon/\varepsilon_0)^2 = 0.5$.

The appearance of bends in the slopes of the formed wide peak (Figs. 3e, 4e, and 5) is a surprising effect. Since physical reasons for the appearance of these bends in the slopes of the peak are apparently absent, it was assumed that it is a manifestation of a defect of the NCA approach. To verify this assumption, we considered a simple model of the summation of two noninteracting peaks, $\bar{G}''_{\pm}(\nu)$, whose maxima are closer to each other than the widths of these peaks. According to Eq. (63), such a system of two peaks in the NCA for one-dimensional inhomogeneities at $k_c = 0$ is described by the expressions

$$\bar{G}''_{\pm}(\nu, k) = \begin{cases} \dfrac{1}{2\pi}\dfrac{1}{2\sigma^2}\sqrt{(2\sigma)^2 - \left(\xi \pm \dfrac{\xi_0}{2}\right)^2}, & \left|\xi \pm \dfrac{\xi_0}{2}\right| \le 2\sigma, \\ 0, & \left|\xi \pm \dfrac{\xi_0}{2}\right| > 2\sigma, \end{cases} \tag{93}$$

where ξ_0 is the spacing between the peaks. In this case, according to Eqs. (62), the exact Green's functions at $k_c = 0$ for one-dimensional inhomogeneities are given by the formula

$$\bar{G}''_{\pm}(\nu, k) = \frac{\pi}{(2\pi)^{5/2}\sigma}\exp\left[-\frac{1}{2\sigma^2}\left(\xi \pm \frac{\xi_0}{2}\right)^2\right]. \tag{94}$$

These functions and envelopes of their sums at $\xi_0 = \sigma/2$ are shown in Fig. 6 by the dashed and solid lines, respectively. It can be seen that the sum of the exact (Gaussian) peaks gives the smooth slopes of the resulting peak (Fig. 6b), whereas the sum of the peaks corresponding to the NCA is responsible for the appearance of bends in the slopes of the resulting peak (Fig. 6a). This model obviously does not reproduce all features of really interacting peaks (induced by this interaction) shown in Figs. 3–5. However, it certainly shows that bends in the slopes of the wide peak in Figs. 3e, 4e, and 5 are really due to the defect of the NCA approach. This defect is not manifested in other panels of Figs. 3 and 4, where the spacing between the peaks is still large (panels a–d) or is zero (panel f). The comparison of Figs. 3e, 4e, and 5 shows that the defect of the NCA is most pronounced for small k_c values (Fig. 5, $\kappa_c = 0.8 \times 10^{-3}$) and is gradually smoothed with an increase in this parameter, i.e., with an increase in the damping of waves (Fig. 3e, $\kappa_c = 0.8 \times 10^{-2}$ and Fig. 4e, $\kappa_c = 0.8 \times 10^{-1}$).

According to Eqs. (78), the off-diagonal elements of the Green's functions have the same frequency dependence. For this reason, when analyzing the off-diagonal elements, we calculated only one quantity $G_{ij}(\omega)$ related to G_{mu} and G_{um} as

$$G_{ij}(\omega) = \sqrt{\frac{\mu}{\alpha}}G_{mu}(\omega) = \sqrt{\frac{\alpha}{\mu}}G_{um}(\omega). \tag{95}$$

The real and imaginary parts of the renormalized off-diagonal element $G_{ij}(\omega)$ at various relations between the mean value ε and rms fluctuation Δε of the coupling parameter are shown in Fig. 7. Since $G_{ij}(\omega) \sim \varepsilon$, with an increase in Δε and a decrease in ε, the amplitudes of both $G'_{ij}(\omega)$ and $G''_{ij}(\omega)$ decrease and vanish in the limit $\varepsilon \longrightarrow 0$. It can be seen in Fig. 7b that, with an increase in Δε, the peaks of the imaginary part of off-diagonal elements, as well as the peaks of the diagonal elements in Figs. 3 and 4, first approach each other and are broadened (thin solid, dashed, and dash-dotted lines). However, the seeming peak "repulsion" effect is observed with a further increase in Δε. In the sum of the overlapping broadened peaks of different signs, the inner parts of these peaks cancel each other, whereas their outer parts do not cancel, which leads to an increase in the spacing between their uncompen-

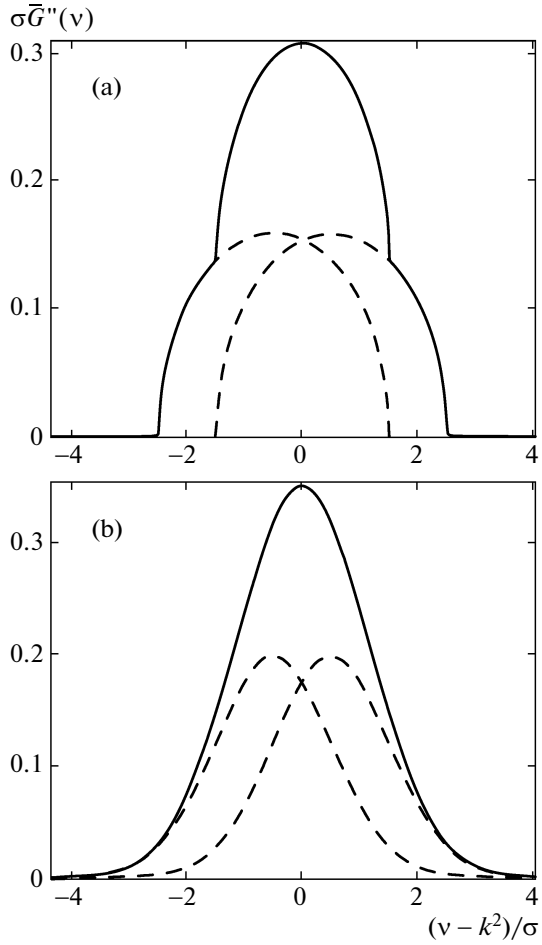

Fig. 6. (Solid curve) Envelope of (dashed curves) two noninteracting resonance peaks corresponding at $\kappa_c = 0$ to (a) the noncrossing correlation approximation and (b) exact summation of the series of the Green's functions.

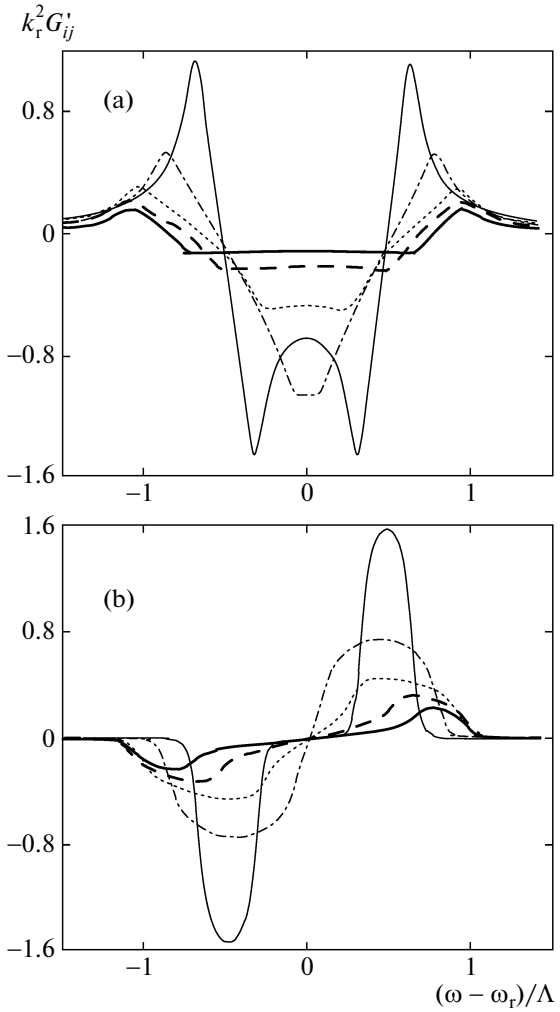

Fig. 7. (a) Real and (b) imaginary parts of the off-diagonal element of the matrix Green's function at $\kappa_c = 0.8 \times 10^{-2}$ and $(\varepsilon/\varepsilon_0)^2/(\Delta\varepsilon/\varepsilon)^2 =$ (thin solid curves) 0.95/0.05, (dash-dotted curves) 0.8/0.2, (dotted curves) 0.5/0.5, (dashed curves) 0.25/0.75, and (thick solid curves) 0.1/0.9.

sated parts. The manifestation of this effect is also enhanced by the aforementioned defect of the NCA, which distorts the shape of approaching peaks.

5. CONCLUSIONS

The self-consistent approximation (noncrossing correlation approximation) has been developed for the case of an arbitrary relation between the mean value ε and rms fluctuation $\Delta\varepsilon$ of the coupling parameter between two wave fields of different physical natures. For definiteness, we study a model problem corresponding to the interaction between spin and elastic waves.

Since the mean value ε of the coupling parameter is nonzero, the initial Green's function $\hat{G}_0(\mathbf{x}, \mathbf{x}_0)$ is a matrix function and describes coupled magnetoelastic waves in a homogeneous medium. Thus, in contrast to the single-field situation, as well as to the purely stochastic interaction between the wave fields ($\varepsilon = 0$, $\Delta\varepsilon \neq 0$) considered in [6–8], the Green's function formalism in this work has been developed against the background of the initial system of coupled wave fields. As a result, each element of the averaged matrix Green's function $\hat{\bar{G}}(\mathbf{x}, \mathbf{x}_0)$ in the generalized Dyson equation is expressed in terms of all four elements of the matrix operator $\hat{Q}(\mathbf{x}, \mathbf{x}_0)$. The generalization of the NCA to this situation leads to the system of four coupled integral equations for the elements of the mass operator in the $\mathbf{k}$ space, which is reduced to the system of three coupled integral equations for the normalized spin, $M_\mathbf{k}$, elastic, $U_\mathbf{k}$, and off-diagonal, $T_\mathbf{k}$, mass operators.

The developed NCA approach has been used to study the diagonal, $\bar{G}_{mm}(\omega, k)$ and $\bar{G}_{uu}(\omega, k)$, and off-diagonal, $\bar{G}_{mu}(\omega, k)$ and $\bar{G}_{um}(\omega, k)$, elements of the averaged

tensor Green's function $\hat{\bar{G}}(\omega, k)$ of the coupled magnetoelastic waves at the magnetoelastic resonance point $k = k_r$, which corresponds to the crossing point of the unperturbed dispersion curves of the spin and elastic waves. The dependence of the shape of these functions on the ratio of the mean value ε and rms fluctuation $\Delta\varepsilon$ of the coupling parameter has been analyzed throughout the entire range of this ratio under the condition of the conservation of the sum of their squares ($\varepsilon^2 + (\Delta\varepsilon)^2 = \varepsilon_0^2$). Thus, we have studied the effect of all intermediate degrees of disorder of the coupling parameter from the completely ordered case ($\varepsilon = \varepsilon_0$, $\Delta\varepsilon = 0$) to the complete randomization of this parameter ($\varepsilon = 0$, $\Delta\varepsilon = \varepsilon_0$). With an increase in $\Delta\varepsilon$, the width of both resonance peaks in the imaginary parts of the diagonal functions $\bar{G}''_{mm}(\omega)$ and $\bar{G}''_{uu}(\omega)$ increase, the peaks approach each other and are joined into one wide peak. A fine structure appears on the tops of wide peaks already at $(\Delta\varepsilon/\varepsilon_0)^2 > 0.25$–$0.40$: a narrow resonance appears in the $\bar{G}''_{mm}(\omega)$ dependence and a narrow antiresonance appears in the $\bar{G}''_{uu}(\omega)$ dependence. Depending on the k_c value, this fine structure can hold for the case of full randomization or can disappear at $\varepsilon = 0$ in one or both Green's functions. The amplitudes of the peaks in the real and imaginary parts of the off-diagonal Green's functions $\bar{G}''_{mu}(\omega)$ and $\bar{G}''_{um}(\omega)$ decrease with an increase in $\Delta\varepsilon$ and vanish at $\Delta\varepsilon = \varepsilon_0$; i.e., the cross excitation of spin and elastic elements of magnetoelastic oscillations in the completely stochastic system is absent.

It has been shown that the equality of the spin and elastic components of magnetoelastic waves at the crossing resonance point, $\bar{G}''_{mm}(\omega_r) = \bar{G}''_{uu}(\omega_r)$, which was found in [8] for the case $\varepsilon = 0$, is valid for any relations between ε and $\Delta\varepsilon$. To satisfy this equality, the fine structure appears: a narrow maximum in the smaller function (at $\omega \neq \omega_r$) coincides with a narrow minimum in the larger function (at $\omega \neq \omega_r$). The other relation found in [8]—the proportionality of the ratio $\bar{G}_{mm}(\omega_r)/\bar{G}_{uu}(\omega_r)$ at $k_c = 0$ to the ratio of the velocities of the respective waves—is also valid for any relations between ε and $\Delta\varepsilon$.

In this work, the first crossing of dispersion curves, which corresponds to the inequality $\bar{G}''_{mm}(\omega) < \bar{G}''_{uu}(\omega)$ at $\omega \neq \omega_r$, has been considered. At the point of the second crossing, $\bar{G}''_{mm}(\omega) > \bar{G}''_{uu}(\omega)$ and the fine-structure pattern changes to opposite: narrow resonance and narrow antiresonance appear in the $\bar{G}''_{uu}(\omega)$ and $\bar{G}''_{mm}(\omega)$ dependences, respectively. The crossing resonance of spin and elastic waves has been studied in this work. Relations for the crossing resonance of waves or quasiparticles of another nature will have another form. However, the general character of the variation of dynamic susceptibilities with an increase in $\Delta\varepsilon$ and a decrease in ε should remain unchanged: the width of peaks in the imaginary parts of the diagonal elements of Green's functions of coupled wave fields increases; the peaks approach each other and are joined into one wide peak whose width is proportional to $\Delta\varepsilon$; a fine structure in the form of narrow resonance at the vertex of the smallest diagonal element of the Green's functions and narrow antiresonance at the vertex of the largest element is formed; the peaks of the fine structure is broadened with an increase in k_c and disappears at large k_c values; the imaginary parts of the diagonal elements of the Green's function of wave fields at the point of crossing of the dispersion curves $k = k_r$, $\omega = \omega_r$ are equal to each other; and the amplitudes of the off-diagonal elements of the Green's function vanish in the limit $\varepsilon \longrightarrow 0$.

The disadvantages of the NCA approach have also been analyzed in application to the systems of coupled wave fields. In these systems, the Green's functions of both fields in the crossing resonance region are split into two resonance peaks, which approach each other and are joined into one peak with a decrease in ε and an increase in $\Delta\varepsilon$. In contrast to the exact Green's functions, the peaks of the Green's functions in the NCA are described by function (63) rather than by a Gaussian function. Owing to this circumstance, a spurious effect of the appearance of additional bends distorting the shape of these peaks occurs in the slopes of the peaks of the Green's functions calculated in the NCA when the peaks approach each other at distances smaller than their widths. These distortions decrease and disappear with an increase in k_c.

The experimental detection of the effects predicted in this work would be of most interest for media with a small k_c value and with a quite large excess of the velocity of waves of one field over the velocity of waves of the other field at $k = k_r$. The former property results in small widths of the lines and the latter property is responsible for large amplitudes of resonance and antiresonance peaks of the fine structure.

ACKNOWLEDGMENTS

This work was supported by the Presidium of the Russian Academy of Sciences (program no. 24.29), by the Dynasty Foundation (Program for Support of Young Scientists), by the Federal Target Program (state contract no. 14.B37.21.0730), and by the Special Program of the Ministry of Education and Science of the Russian Federation for the Siberian Federal University.

REFERENCES

1. R. C. Bourret, Nuovo Cimento **26**, 1 (1962).
2. S. M. Rytov, Yu. A. Kravtsov, and V. I. Tatarskii, *Principles of Statistical Radiophysics*, Volume 2: *Correlation*

Theory of Random Processes (Nauka, Moscow, 1978; Springer-Verlag, Berlin, 1988).

3. V. A. Ignatchenko and L. I. Deich, Phys. Rev. B: Condens. Matter **50**, 16364 (1994).
4. L. I. Deich and V. A. Ignatchenko, JETP **80** (3), 478 (1995).
5. L. I. Deich and A. A. Lisyansky, Phys. Lett. A **220**, 125 (1996).
6. V. A. Ignatchenko and D. S. Polukhin, Solid State Phenom. **168–169**, 101 (2011).
7. V. A. Ignatchenko and D. S. Polukhin, Solid State Phenom. **190**, 51 (2012).
8. V. A. Ignatchenko and D. S. Polukhin, JETP **116** (2), 206 (2013).
9. V. A. Ignatchenko, M. V. Erementchouk, A. A. Maradudin, and L. I. Deych, Phys. Rev. B: Condens. Matter **59**, 9185 (1999).
10. V. A. Ignatchenko and V. A. Felk, Phys. Rev. B: Condens. Matter **74**, 174415 (2006).
11. A. I. Akhiezer, in *Abstracts of Papers of the Workshop on Physics of Magnetic Phenomena, Moscow, Russia, May 23–31, 1956* (Metallurgizdat, Sverdlovsk, 1956).
12. E. A. Turov and Yu. P. Irkhin, Fiz. Met. Metalloved. **3**, 15 (1956).
13. A. I. Akhiezer, V. G. Bar'yakhtar, and S. V. Peletminskii, Sov. Phys. JETP **8**, 157 (1958).
14. C. Kittel, Phys. Rev. **110**, 835 (1958).
15. A. I. Akhiezer, V. G. Bar'yakhtar, and M. I. Kaganov, Sov. Phys.—Usp. **3** (4), 567 (1960).
16. A. I. Akhiezer, V. G. Bar'yakhtar, and S. V. Peletminskii, *Spin Waves* (Nauka, Moscow, 1967; North-Holland, Amsterdam, The Netherlands, 1968).
17. V. V. Lemanov, in *Physics of Magnetic Dielectrics*, Ed. by G. A. Smolenskii (Nauka, Leningrad, 1975), p. 85 [in Russian].
18. A. B. Migdal, Sov. Phys. JETP **7**, 996 (1958).
19. D. Pines, *The Many-Body Problem* (W. A. Benjamin, New York, 1961).
20. D. Pines, in *Polarons and Excitons*, Ed. by C. G. Kuper and G. D. Whitfield (Plenum, New York, 1963), p. 155.
21. R. Puff and G. Whitfield, in *Polarons and Excitons*, Ed. by C. G. Kuper and G. D. Whitfield (Plenum, New York, 1963), p. 171.
22. A. A. Abrikosov, L. P. Gorkov, and I. E. Dzyaloshinski, *Methods of Quantum Field Theory in Statistical Physics* (Fizmatgiz, Moscow, 1962; Dover, New York, 1975).
23. R. H. Kraichnan, J. Math. Phys. **2**, 124 (1961).
24. V. I. Klyatskin, *Stochastic Equations through the Eye of the Physicist* (Elsevier, Amsterdam, The Netherlands, 2005; Fizmatlit, Moscow, 2008), Vol. 1.
25. H. Bruus and K. Flensberg, *Introduction to Many-Body Quantum Theory in Condensed Matter Physics* (Ørsted Laboratory, Niels Bohr Institute, University of Copenhagen, Microelectronic Center, Technical University of Denmark, Copenhagen, Denmark, 2002).
26. M. V. Sadovskii, *Diagrammatics: Lectures on Selected Problems in Condensed Matter Theory* (Ural Branch of the Russian Academy of Sciences, Yekaterinburg, 2005; World Scientific, Singapore, 2006).
27. Yu. A. Firsov, *Polarons* (Nauka, Moscow, 1975) [in Russian].
28. N. V. Tkach and R. B. Fartushinskii, Phys. Solid State **45** (7), 1347 (2003).
29. N. A. Armand and V. N. Sekistov, Izv. Vyssh. Uchebn. Zaved., Radiofiz. **23**, 555 (1980).
30. N. N. Zernov, Izv. Vyssh. Uchebn. Zaved., Radiofiz. **25**, 520 (1982).
31. V. N. Sekistov, Radiotekh. Elektron. **28** (7), 1262 (1983).
32. V. A. Ignatchenko and V. A. Felk, Phys. Rev. B: Condens. Matter **71**, 094417 (2005).
33. P. Soven, Phys. Rev. [Sect.] B **156**, 809 (1967).
34. D. W. Taylor, Phys. Rev. [Sect.] B **156**, 1017 (1967).
35. B. Velický, S. Kirkpatrick, and H. Ehrenreich, Phys. Rev. **175**, 747 (1968).
36. F. Yonezawa and K. Morigaki, Suppl. Prog. Theor. Phys. **53**, 1017 (1973).
37. R. J. Elliott, J. A. Krumhansl, and P. L. Leath, Rev. Mod. Phys. **46**, 465 (1974).
38. G. Brown, V. Celli, M. Haller, A. Maradudin, and A. Marvin, Phys. Rev. B: Condens. Matter **31**, 4993 (1985).
39. I. M. Lifshitz, S. A. Gredeskul, and L. A. Pastur, *Introduction to the Theory of Disordered Systems* (Nauka, Moscow, 1982; Wiley, New York, 1988).
40. J. M. Ziman, *Models of Disorder: The Theoretical Physics of Homogeneously Disordered Systems* (Cambridge University Press, Cambridge, 1979; Mir, Moscow, 1982).
41. E. N. Economou, *Green's Functions in Quantum Physics* (Springer-Verlag, Berlin, 2006).
42. E. Schlomann, J. Phys. Chem. Solids **6**, 257 (1958).

Translated by R. Tyapaev